ON THE CONTRIBUTION OF THE MAGNETIC FIELD ON THE RECIPROCATING COMPRESSOR NOISE

Gustavo Myrria
Arcanjo Lenzi
Universidade Federal de Santa Catarina
gustavo.myrria@lva.ufsc.br
arcanjo@lva.ufsc.br

Abstract. One of the main noise sources in the reciprocating compressor used in domestic refrigeration system is the electric motor. Through this electrical machine the necessary energy to the piston compress the refrigeration fluid is transferred to the reciprocating compressor. The main noise and vibration source in an electrical machine is the actuation of the electromagnetic field present during the machine operation. The electromagnetic field produces excitations that induce vibration on the structural elements of the compressor, such as stator tooth, windings among others. The objective of this work is to model the magnetic field, obtain the magnetic excitations and analyze the contribution of this source on the compressor noise. A finite element model of the magnetic system is used to obtain the magnetic field and through the Maxwell Tensor the forces are acquired. A numerical model of the mechanical system was constructed to get the dynamic response of the system as well. The excitations obtained were close to the analytical expectations and forced the stator to vibrate in some specific frequencies. The knowledge of which frequency the stator core is excited is important since these forces could be close to the resonance frequency of other compressor component.

Keywords: noise, induction motor, FEM

1. INTRODUCTION

One of the main source of vibration and noise on hermetic compressors is the induction motor (Carneiro, 2008; Carmo, 2001). The vibration and noise sources of these machines can be divided in three categories: mechanical, aerodynamical and magnetic (Gieras *et al.*, 2006). The aerodynamic vibration and noise is associated with flow of ventilating air through or over the motor. The mechanical sources are associated with the mechanical assembly. Finally, the electromagnetic vibration and noise source are associated to parasitic effects due to higher space and time harmonics, eccentricity, magnetic saturation and magnetostrictive expansion of the core laminations.

Even though the induction motor is recognized as one of the main vibration and noise source on the hermetic compressor, only few works were committed to investigate this phenomenon. In his book about reciprocating compressors, Soedel (2007) give some information of the critical frequencies of the induction machine. Paiotti (2002) modeled the induction machine of a commercial hermetic compressor using FEM and obtained the magnetic forces. From this work it was concluded that the normal components of the magnetic forces have higher magnitudes than the tangential components. It was also found that the tangential forces become more relevant with the increasing of the frequency.

The objective of this work is to obtain the mechanical excitations that results from the presence of the magnetic field during the operation of the induction motor. The numerical model was constructed using the finite element method (FEM). Through this numerical model the magnetic distribution is obtained and then the resultant forces through the Maxwell Tensor Method.

2. MATHEMATICAL METHODOLOGY

As it was cited before, the noise produced by the operation of electric motors is caused by three sources: electromagnetic sources, mechanic sources and aerodynamic sources. In this work the electromagnetic and the structural systems were modeled as can be seen in the topics below.

2.1 Electromagnetic modelling

The electromagnetic field produced by the electric excitation can be obtained from using of the Maxwell equations (Roivainen, 2009). These equations is a set of laws that in addition with constitutive laws of the magnetic material can rule the electromagnetic phenomena such as the propagation of the electromagnetic waves and the magnetic field generated by a permanent magnet. The equations that characterize the electromagnetic problem are shown below (Kalluf *et al.*, 2010):

$$\nabla \times \mathbf{H} = \mathbf{J} + \frac{\partial \mathbf{D}}{\partial t} \tag{1}$$

$$\nabla \cdot \mathbf{B} = 0 \tag{2}$$

$$\nabla \times \mathbf{E} \;=\; \frac{\partial \mathbf{B}}{\partial t} \tag{3}$$

where $\mathbf{H}$ is the magnetic field, $\mathbf{B}$ is the magnetic flux density, $\mathbf{E}$ is the electric field, $\mathbf{J}$ is the electric current density and $\mathbf{D}$ is the electric flux density. The constitutive relations of the magnetic material are:

$$\mathbf{B} \;=\; \mu \mathbf{H} \tag{4}$$
$$\mathbf{J} \;=\; \sigma \mathbf{E} \tag{5}$$

where μ is the magnetic permeability and σ is the electric conductivity. In this work is used the $\mathbf{A}$-formulation, where the magnetic vector potential ($\mathbf{A}$) and the scalar electric potential (ϕ) are described as:

$$\mathbf{B} \;=\; \nabla \times \mathbf{A} \tag{6}$$
$$\mathbf{E} \;=\; -\nabla \phi. \tag{7}$$

For the frequency range that is encountered our problem, the polarization and displacement currents are assumed to be small compared with the conductive currents in the conductor (Arkkio, 1987), then:

$$\frac{\partial \mathbf{D}}{\partial t} << \mathbf{J}. \tag{8}$$

Manipulating the equations described above the magnetic vector potential and the electric scalar potential can be obtained by (Arkkio, 1987):

$$\nabla \times \left(\frac{1}{\mu} \nabla \times \mathbf{A} \right) + \sigma \frac{\partial \mathbf{A}}{\partial t} + \sigma \nabla \phi = 0 \tag{9}$$

$$\nabla \cdot \left(\sigma \frac{\partial \mathbf{A}}{\partial t} \right) + \nabla \cdot (\sigma \nabla \phi) = 0. \tag{10}$$

In this work a two-dimensional analysis was applied. This simplification can be used when the electrical machine is homogenous in the axial direction and of which the axial dimension is sufficiently large compared to its diameter (van der Giet *et al.*, 2008). Using this approach it is assumed that the geometry and the material quantities don't vary significantly along the axial direction of the motor. Assuming that the xy-plane is cross-section plane of the induction motor and the z axis is in parallel to the axial direction of the motor, the vector potential and the current density are given by:

$$\mathbf{A} = A(x, y, t)\mathbf{e_z} \tag{11}$$
$$\mathbf{J} = J(x, y, t)\mathbf{e_z} \tag{12}$$

where x and y are the cartesian spatial coordinates and $\mathbf{e_z}$ is the unit vector parallel to the z-axis.

The uniqueness of the solution requires that a value must be given to the divergence of the vector potential. In solving the Equations 9 and 10, the following boundary conditions are applied (Maliti, 2000):

1. **Dirichlet condition**: $(A = \alpha_0)$, i.e., the vector potential is constant on the external boundary Γ of the cross-sectional domain Ω. In this work $A = \alpha_0 = 0$ was selected.

2. **Neumann condition**:

$$\frac{\partial A}{\partial n} = 0 \tag{13}$$

where n is a unit vector normal to the external boundary Γ.

3. **Periodicity condition**:

$$A(r, \theta) = A(r, \theta + \theta_0) \tag{14}$$

where r and θ are cylindrical coordinates, and θ_0 is the period of A.

The magnetic density distribution causes a mechanical excitation on the structure. There are several methods to obtain these forces generated by the magnetic density. One of the most popular is the Maxwell Stress Tensor. This method is applied on the edge between iron and air gives a magnetic force density which can be written as (da Costa Neves *et al.*, 1999):

$$\sigma = \frac{1}{\mu_0} \left[(\mathbf{n} \cdot \mathbf{B}) \mathbf{B} - \frac{1}{2} B^2 \mathbf{n} \right] \tag{15}$$

where μ_0 is the permeability of the air, $\mathbf{B}$ is the air side magnetic density and $\mathbf{n}$ is the vector normal to iron. Once the mechanical forces are obtained they are transfered to a structural model as shown in the Fig. 1.
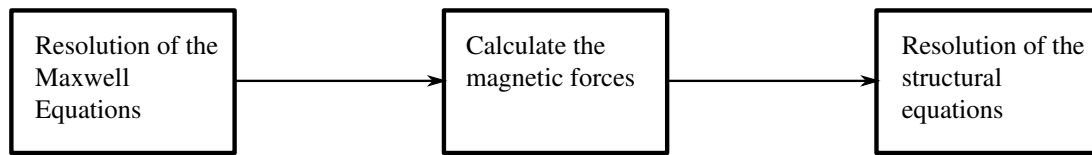
Figure 1: Simulation process adopted in this work

2.2 Structural modelling

The magnetic force obtained through the electromagnetic model is imposed as an excitation for the structure-dynamic simulation, which is governed by:

$$(\mathbf{K} - \omega^2 \mathbf{M}) = \mathbf{F}, \tag{16}$$

where $\mathbf{K}$ is the stiffness matrix, $\mathbf{M}$ is the mass matrix, $\mathbf{u}$ is the time harmonic displacement vector, and $\mathbf{F}$ is the load vector which is computed be projecting the electromagnetic forces from the 2D electromagnetic mesh to a 3D structure dynamic mesh (van der Giet *et al.*, 2008).

3. Results and discussion

As cited before, a model using the FEM was developed to represent the electromagnetic phenomena and the resultant mechanic forces. The commercial software ANSYS Maxwell was used to construct and to solve the equations. The 2D model developed is shown in the Figure 2. Considering the symmetry of the induction machine, only half of the motor was considered and an antiperiodicity condition was assumed. As a boundary condition is assumed $\nabla \cdot \mathbf{A} = 0$ at the external boundary of the domain. The moving band technique (Sadowski *et al.*, 1992) was also implemented to model the rotation of the rotor in relation to the stator.
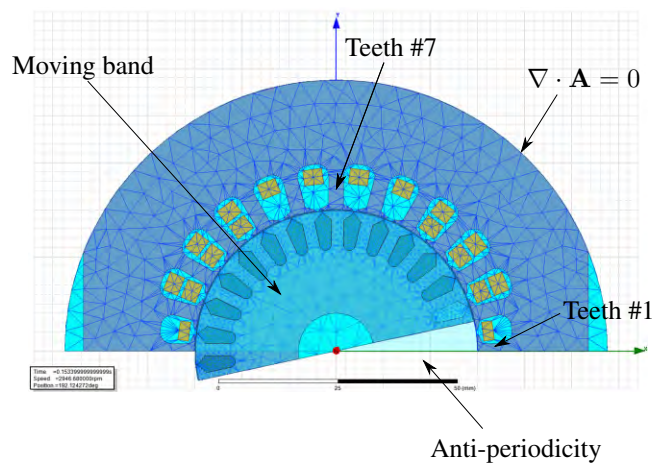

Figure 2: Induction machine model developed by the using of FEM.

The main characteristics of the numerical model of the induction motor are presented in the Table 1.

Table 1: Main characteristics of the numerical model of the induction machine.

Number of stator slots	N_s	24
Number of rotor slots	N_r	28
Pole pair number	p	1
Slip	n	0.018
Source frequency	f_1	50 Hz
Number of elements		7254
Total period of analysis	T	0.2 s
Time step	Δt	5e-5 s

A non-linear curve of $\mathbf{B} - \mathbf{H}$ shown in the Figure 3 was used to represent the iron used in the stator and the rotor. From the nonlinear relation of the curve $\mathbf{B} - \mathbf{H}$ arises spatial harmonics of the $\mathbf{B}$ along the gap due to magnetic saturation (Maliti, 2000). The bars of the rotor were modeled with aluminum material and the coil with copper.
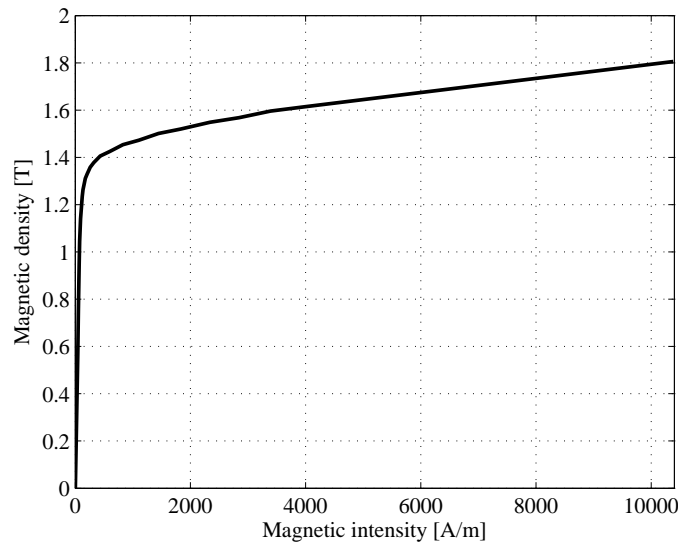
Figure 3: Nonlinear relation between **B** and **H** of Iron of stator and rotor.

The circuit equations that feed the coils of the FEM model were considered and a strong coupling was implemented. The electric circuit used in the analysis is shown in the Figure 4.
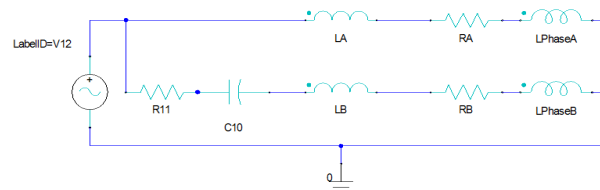

Figure 4: Electric circuit used in the analysis.

After the electromagnetic model is developed, the model is processed. With the results of the magnetic field on the electromagnetic model, the magnetic forces are obtained with the using of the Eq. 15. The results of main characteristics of the motor are shown in the Fig. 5. These results were close to the experimental test results. From the experiments it was obtained that the maximum torque is 4.7 kgf·cm with a current of 1.1 A, which are very close to the numerical results. The Figure 6 shows the equipotential lines of **A** and the rotational movement of the rotor for a instant. Applying the Maxwell Tensor Method on the tooth #1 and #7 the results of mechanical stress are shown in the Figure 7. Through the Figure 7a can be seen that the resulting stress on the tooth are similar, despite of the expected phase between them. It can be also observed that they present some harmonics which are summed to the fundamental harmonic component. The Figure 7b shows the magnitude of the stress in the frequency domain. As the time domain it is observed that the stress on both teeth is very similar. It is also noted significant stress magnitudes for the resonance frequencies 100 Hz, 1250 Hz, 2500 Hz and their harmonics. These harmonics were expected to be encountered with the using of the analytical procedure (C. Schlensok and Hameyer;, 2007). A summary of the resonance frequencies for induction machines and the respective results for the studied electrical machine are presented in the Table 2.

Table 2: Predicted ressonance frequencies of the magnetic forces.

Double stator frequency	$2f_1$	100 Hz
1st rotor-slot harmonic	$N_r n$	1375.1 Hz
2nd rotor-slot harmonic	$2N_r n$	2750.2 Hz
1st stator-slot harmonic	$N_s n$	1178.6 Hz
Modulated 1st rotor-slot harmonic	$N_r n + 2f_1$	1475.1 Hz
Modulated 1st rotor-slot harmonic	$N_r n - 2f_1$	1275.1 Hz
Modulated 2nd rotor-slot harmonic	$2N_r n + 2f_1$	2850.2 Hz
Modulated 2nd rotor-slot harmonic	$2N_r n - 2f_1$	2650.2 Hz

It may be noted that the stress with more significant magnitudes were very close to the predicted resonance frequencies.
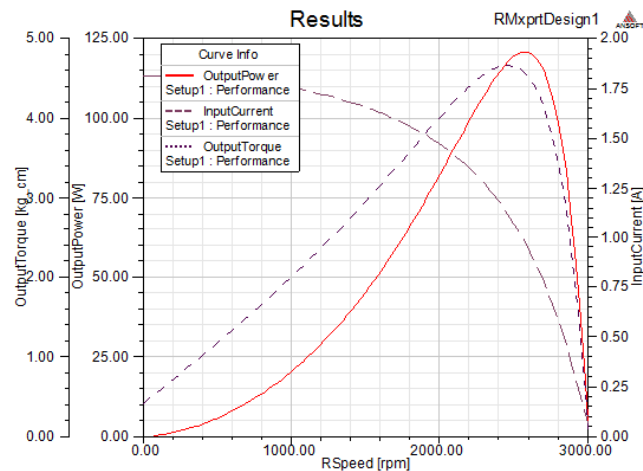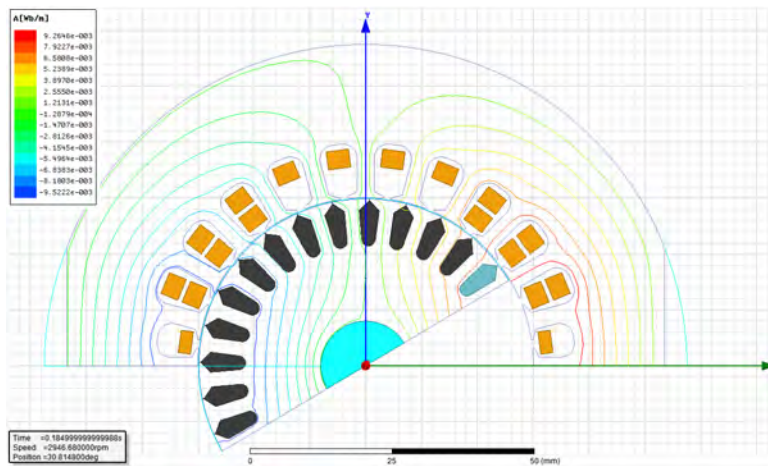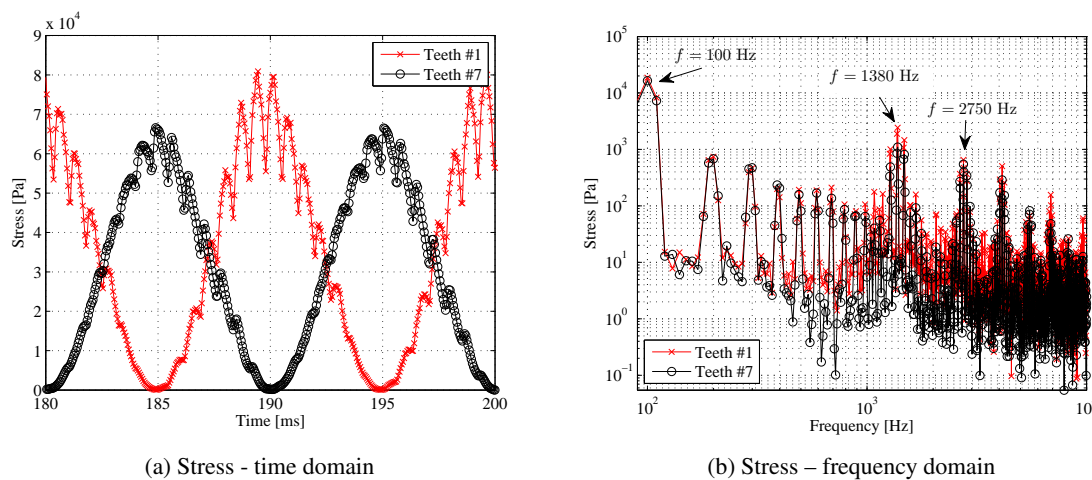
Figure 5: Results of the main characteristics of the induction motor.

Figure 6: Equipotential lines of **A** obtained by the FEM model.

(a) Stress - time domain
(b) Stress – frequency domain

Figure 7: Results of stress obtained from FEM model.

This information is relevant because it is desired to avoid excitations with frequencies close to the structural resonances.

The next step after obtaining the magnetic forces that are acting on the tooth is transferring them to a structural model. For the mechanical model the software COMSOL was used. The model of the laminated stator is presented in the Fig. 8. A equivalent orthotropic property informed by David Franck (2010) was used and the it is shown in the Tab. 3.

In order to validate the numerical model an experimental frequency response function (FRF) was acquired. A shaker was used to insert vibrational energy on the stator. The transmitted force and the acceleration were acquired by an impedance head and an accelerometer, respectively. The Fig. 9a shows the experimental setup. The resulting FRF is shown in the Fig. 9b.

Table 3: Properties of the equivalent material of the laminated stator.

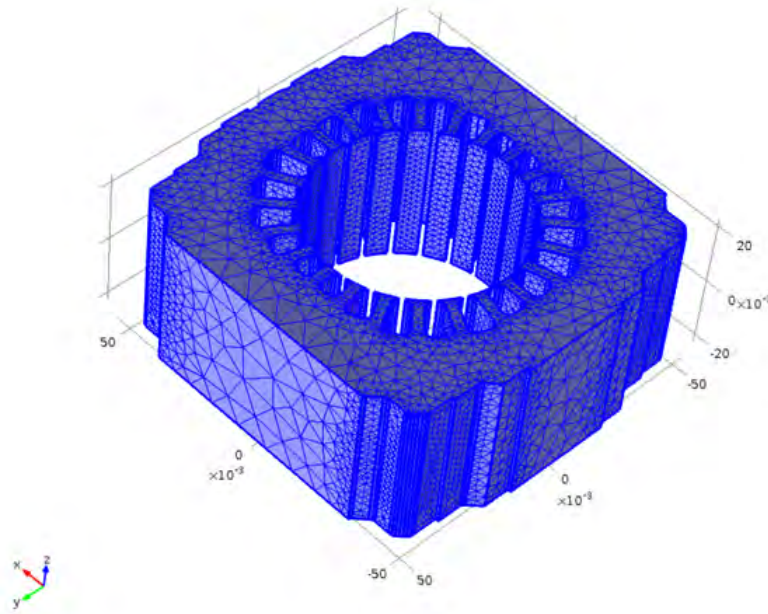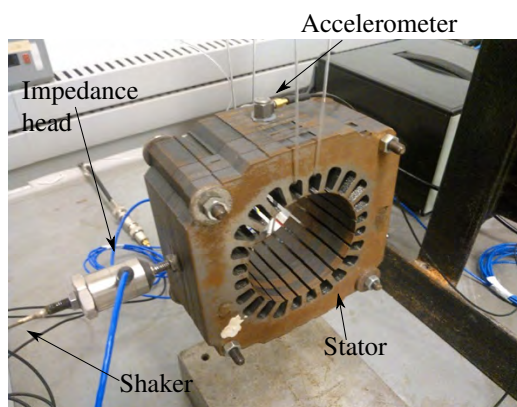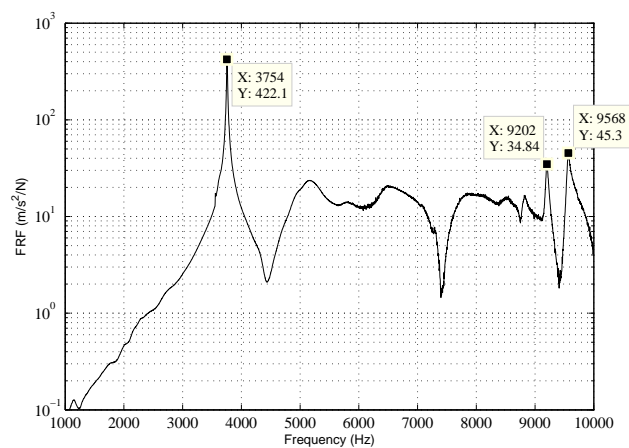|	
E_x (GPa)	212.7
E_z (Gpa)	26.3
ν_{xy}	0.4
ν_{xz}	0.14
G_{xz} (GPa)	90.2

Figure 8: Numerical model of the laminated stator.

(a) Experimental setup

(b) FRF from experiments.

Figure 9: (a) Experimental setup of the test and (b) resulted FRF of the laminated stator.

The results of the structural resonance frequencies for the in-plane modes obtained from the numerical model were compared to the ones obtained experimentally in the Tab. 4. Additionally the expected natural frequencies from the analytical model proposed by Anwar (2000) is also included. It can be seen a good agreement of the resonance frequencies. The knowledge of this information is important to the designer of the electrical machine avoid excitations with resonance frequencies close to the structural ones.

Table 4: Comparison of the in-plane structural ressonance frequencies of the laminated stator.

Mode	Analytical	Nummerical	Experimental
1	3881 Hz	3717 Hz	3754 Hz
2	9921 Hz	9461 Hz	9568 Hz

4. CONCLUSIONS

The magnetic excitations originated from the magnetic field produced during the operation of the induction machine were numerically obtained. The field equations and the circuit equations were coupled and the 2D FEM was used to model the operation of induction motor. The frequencies of the magnetic forces obtained by the Maxwell Tensor were compared to the analytical methods and a good agreement was observed. A structural model was also developed to represent the laminated stator. To represent the laminated stator an orthotropic equivalent material was used. Comparing the numerical results to experimental results it was noted a good concordance. This numerical model will be used to receive the magnetic forces and acquire the dynamic response.

5. REFERENCES

Anwar, M.N.; Husain, O., 2000. "Radial force calculation and acoustic noise prediction in switched reluctance machines". *Industry Applications, IEEE Transactions on*, Vol. 36, No. 6, pp. 1589 – 1597. ISSN 0093-9994. doi: 10.1109/28.887210.

Arkkio, A., 1987. *Analysis of induction motors based on the numerical solution of the magnetic field and circuit equations*. Ph.D. thesis, Helsinki University of Technology.

C. Schlensok, B. Schmülling, M.v.d.G. and Hameyer;, K., 2007. "Electromagnetically excited audible noise - evaluation and optimisation of electrical machines by numerical simulation". *COMPEL*, Vol. 26, pp. 727–742.

Carmo, M.G.V.D., 2001. *Fluxo De Energia Vibratória Do Conjunto Motocompressor Para A Carcaça De Um Compressor Hermético Através Das Molas De Suspensão*. Master's thesis, UFSC.

Carneiro, E.B., 2008. *Aplicação De Absorvedores Tipo Membrana Em Cavidades E Filtros Acústicos*. Master's thesis, UFSC.

da Costa Neves, C., Carlson, R., Sadowski, N., Bastos, J. and Soeiro, N., 1999. "Forced vibrations calculation in a switched reluctance motor taking into account the viscous damping". In *Electric Machines and Drives, 1999. International Conference IEMD '99*. pp. 110 –112. doi:10.1109/IEMDC.1999.769043.

David Franck, Michael van der Giet, K.H., 2010. "Simulation of acoustic radiation of an ac servo drive". *COMPEL: The International Journal for Computation and Mathematics in Electrical and Electronic Engineering*, Vol. 29 Iss: 4, pp. 1060 – 1069.

Gieras, J., Lai, J. and Wang, C., 2006. *Noise of polyphase electric motors*. Number v. 10 in Electrical and computer engineering. CRC/Taylor & Francis. ISBN 9780824723811. URL http://books.google.com/books?id=Fsz-1hYfMv4C.

Kalluf, F.J.H., Pompermaier, C., Ferreira da Luz, M.V. and Sadowski, N., 2010. "Modelling of a line-start permanent magnet motor using finite element method". In *Power Electronics, Machines and Drives (PEMD 2010), 5th IET International Conference on*. pp. 1 –4. doi:10.1049/cp.2010.0204.

Maliti, K.C., 2000. *Modelling and analysis of magnetic noise in squirrel-cage induction motors*. Ph.D. thesis, Royal Institute of Technology.

Paiotti, L.R., 2002. *Vibrações induzidas pelo Campo Eletromagnético no Estator de Motores de Indução de Compressores Herméticos*. Master's thesis, UFSC.

Roivainen, J., 2009. *Unit-wave response-based modeling of electromechanical noise and vibration of electrical machines*. Ph.D. thesis, HELSINKI UNIVERSITY OF TECHNLOGY. URL http://lib.tkk.fi/Diss/2009/isbn9789512299119/isbn9789512299119.pdf.

Sadowski, N., Lefevre, Y., Lajoie-Mazenc, M. and Cros, J., 1992. "Finite element torque calculation in electrical machines while considering the movement". *Magnetics, IEEE Transactions on*, Vol. 28, No. 2, pp. 1410 –1413. ISSN 0018-9464. doi:10.1109/20.123957.

Soedel, W., 2007. *Sound and vibration of positive displacement compressors*. CRC Press.

van der Giet, M., Schlensok, C., Schmülling, B. and Hameyer, K., 2008. "Comparison of 2-D and 3-D Coupled Electromagnetic and Structure-Dynamic Simulation of Electrical Machines". *IEEE Transactions on Magnetics*, Vol. 44, No. 6, pp. 1594–1597. URL http://134.130.107.200/uploads/bibliotest/2008MVDG2D3D.pdf. [2008MVDG2D3D]http://134.130.107.200/uploads/bibliotest/2008MVDG2D3D.pdf.

Gustavo Myrria, Arcanjo Lenzi
On The Contribution Of The Magnetic Field On The Reciprocating Compressor Noise

6. RESPONSIBILITY NOTICE

The authors are the only responsible for the printed material included in this paper.